
Context Preserving Autoregressive Frame Generation for Bounded Video

Anonymous Author(s)

Affiliation
Address
email

Abstract

1 Recently, various video generation methods have been proposed, as diffusion mod-
2 els demonstrate their superior ability to generate high-quality videos. Specifically,
3 autoregressive approaches have been suggested to enable the generation of videos
4 of arbitrary length. However, the methods are not suitable for bounded video
5 generation, as they generate open-ended videos. Moreover, recent methods for
6 bounded video generation rely on flipping frames to satisfy the boundary constraint
7 imposed by the ending frame. However, this approach contradicts the inherent bias
8 of video models to generate frames in forward direction, limiting the generation
9 capability. Accordingly, we propose a novel autoregressive approach for bounded
10 video generation. Specifically, we introduce a context-aware bidirectional denois-
11 ing method that progressively generates frames in both forward and backward
12 directions while considering the frame context. Then, we propose a method to
13 mitigate the context gap between the two directions, to ensure smooth and coherent
14 transition between the sequences. Experimental results demonstrate the superiority
15 of our approach over previous methods. Specifically, as our method aligns with
16 the video model’s forward generation bias, the output videos present more realistic
17 motion dynamics. Moreover, our method outputs frames with enhanced visual
18 quality by maintaining a consistent frame length for model input. More results can
19 be found in our project page¹.

20 **1 Introduction**

21 Recent advances in video diffusion models have revolutionized the video generation method, achiev-
22 ing remarkable visual quality and creative flexibility conditioned by text. The proposed video diffusion
23 models are based on various architectures such as U-Net[2, 3, 10, 24] and transformers[6, 13, 14].
24 Both architectures output high-quality videos with enhanced temporal coherence and semantic
25 alignment. However, they generate an entire video sequence at once, treating the temporal axis as
26 an additional dimension of the diffusion latent vector. This significantly increases computational
27 burden, making long video generation challenging. Accordingly, autoregressive approaches have
28 been suggested, which generate video frames progressively. The methods leverage previous frames as
29 a conditioning factor for later frames, which is able to generate videos with flexible length. This ap-
30 proach facilitates long-range dependencies, allowing for consistent motion propagation throughout the
31 sequence[18, 21, 26]. However, training the video model requires extensive computational resources
32 and access to refined video datasets. To overcome the limitation, training-free methods[11, 17, 22]
33 have recently been proposed to enhance long-range dependencies without requiring enormous training
34 resources. Despite their advantages, these methods primarily focus on open-ended video generation,
35 making them unsuitable for bounded video generation.

¹<https://sites.google.com/view/cpag-video>

36 Bounded video generation refers to the task of
 37 synthesizing a video sequence that adheres to
 38 predefined bounds. This task is essential for
 39 various applications, including video interpola-
 40 tion, video completion, and content extension
 41 while maintaining temporal coherence. Recent
 42 methods[5, 23, 25] proposed to fuse forward and
 43 reversed frames to satisfy the boundary frame
 44 condition. However, existing approaches utilize
 45 frame-flipping techniques, where reversed frames
 46 are synthesized by flipping the generated forward
 47 frames. This introduces inherent limitations, as
 48 flipping the output frames encounters the conflict
 49 to the model’s bias to generate frames in forward
 50 direction. For instance, irreversible motions are
 51 generated with unrealistic dynamics, since the method flips output frames to obtain time-reversal
 52 video sequence. Moreover, the methods have constraints on video length, as they fuse sequences of
 53 fixed length. Specifically, the mismatch of input sequence length between the training and inference
 54 limits the model’s generation capability, as suggested in the prior work [17].

55 To address the limitations, we propose a novel autoregressive approach for bounded video generation.
 56 Specifically, as shown in Fig. 1, our method aims to generate coherent bounded video, considering the
 57 interdependency between the two sequences. The proposed method consists of two parts. First, we
 58 suggest a context-aware bidirectional denoising method. Specifically, inspired by Stein Variational
 59 Gradient Descent (SVGD), we present context gradient that exchanges score information with
 60 neighboring frames. Then, we denoise frames by the diffusion steps, scheduled for bidirectional
 61 generation. Second, we propose a method to reduce the context gap between the two directions. To
 62 be specific, a content generated in each direction may diverge unless the interdependency between
 63 the two sequences is explicitly addressed. Accordingly, we mitigate the context gap by the proposed
 64 frame initialization strategy and the mixing of context gradients. Consequently, our method effectively
 65 guides diffusion process to generate videos with improved consistency while satisfying boundary
 66 conditions. Compared to previous methods based on the frame-flipping technique, our method aligns
 67 with the model’s bias when generating frames in reversal direction. As a result, our method generates
 68 videos with more realistic dynamics. Fig. 2 summarizes a main conceptual difference of our work
 69 compared to the previous approach. Our contributions are summarized as follow:

- 70 • We suggest a novel bidirectional autoregressive approach for bounded video generation,
 71 which aligns with the video model’s forward generation bias.
- 72 • We propose a context gradient which enables to exchange the score information with
 73 neighbor frames, and present a context-aware bidirectional denoising method.
- 74 • We explore the context gap between the two directions, and propose a novel method to
 75 mitigate the context gap to generate coherent videos.
- 76 • We empirically demonstrate the proposed method, highlighting the effectiveness of our
 77 autoregressive approach for bounded video generation.

78 2 Related works

79 2.1 Video diffusion model

80 Recently, many research work consistently demonstrate the superior ability of the diffusion model for
 81 video generation. [2, 3, 6, 14]. Moreover, to address the growing demand for long video generation,
 82 various methods have been proposed, including autoregressive approach that enables the generation of
 83 videos of arbitrary length. Specifically, [21, 26] proposed to obtain autoregressive models by training
 84 with designed objective. However, by the excessive resources for training models, training-free
 85 methods have been proposed. Gen-L-Video[22] proposes temporal co-denoising, which uses the
 86 average of multiple predictions to generate one frame. FreeNoise[17] suggests a novel temporal
 87 attention matrix to retain long-range correlation. FIFO[11] proposes iterative diagonal denoising
 88 to generate video frames in autoregressive manner. Specifically, FIFO suggests latent partitioning

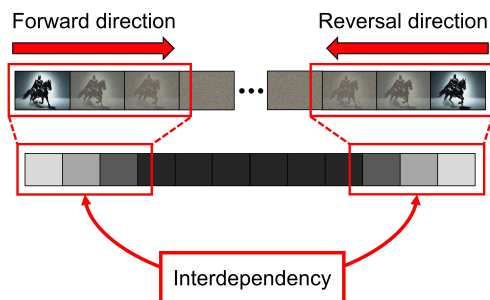


Figure 1: Concept of the proposed bidirectional autoregressive approach, addressing context gap.

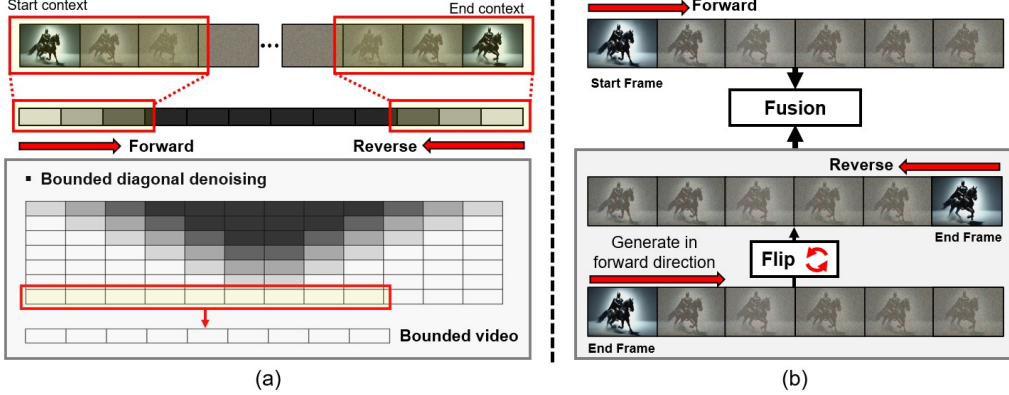


Figure 2: Comparison of our method with previous approach. (a) Proposed autoregressive approach. (b) Previous methods based on flipping frames to generate reversal sequence.

and lookahead denoising to reduce the training-inference gap. However, previous methods generate open-ended videos, which is not suitable for bounded video generation. In this paper, we propose a novel autoregressive method for bounded video generation, which satisfies the boundary conditions while allowing the generation of video in arbitrary length.

2.2 Bounded video generation

With the rise of video diffusion models, various methods have been proposed for bounded video generation. Generative Inbetweening[23] fine-tunes the projection matrix, and interpolate forward and reversed frames. Specifically, it generates reversed frames by rotating the self-attention matrix and flipping the output frames. However, to avoid the computational cost of fine-tuning, training-free methods have emerged. TRF[5] obtains reversed frames by flipping the generated outputs, and linearly interpolates with forward frames. Moreover, authors suggest noise injection for smooth connectivity. ViBiDSmapler[25] proposed a novel diffusion denoising step that combines forward and reversal frame generation process. Specifically, the method denoises the frames in forward direction, and flips the frames to predict noise in reversal direction. Moreover, DDS guidelines[4] is applied to enforce the boundary condition. However, video models are inherently biased to generate frames in forward temporal direction, making such approaches misaligned with the model’s natural behavior. Moreover, they fuse the sequences with fixed length, which constraints the flexibility of video length. As introduced in [17], the difference of input frame length degrades the model’s generation capability. To address the limitation, we propose an autoregressive approach to generate reversed frames by adding more noise in desired direction. Moreover, our method enables to generate videos of arbitrary length with consistent input frame length, which is restricted in the previous methods.

3 Main Contribution

3.1 Key observation: Autoregressive reversed frame generation

Previous methods[5, 23, 25] synthesize reversed videos by flipping frames generated in forward direction, which is counter to the model’s bias. To address the issue, we approach the generation of reversed frame in autoregressive generation. Specifically, inspired by the diagonal denoising[11, 18], we explore a reversed diagonal denoising as shown in Fig. 3, which applies more noise in the preceding frames. This provides an information of future frames to the past frames, enabling the generation of reversed frame without opposing the model’s inherent forward-generation bias.

The results demonstrate that the method successfully generates the reversed frames. As shown in Fig. 3,

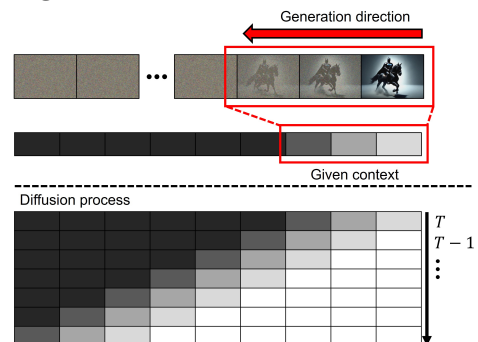


Figure 3: Diffusion time of reversed diagonal denoising. Dark colors refer high noise levels.

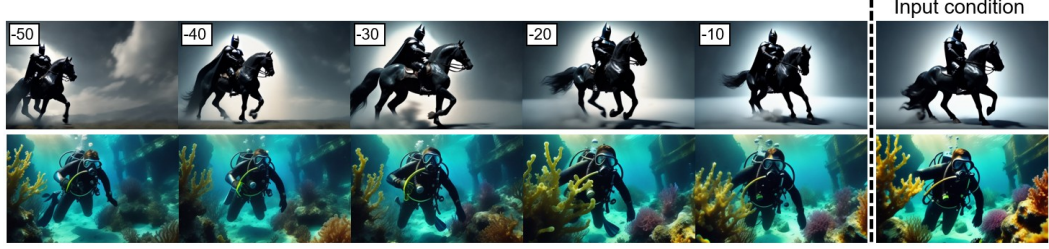


Figure 4: Reversed frame generation by the reversed diagonal denoising. The negative numbers indicate the difference in frame index from the input image.

126 the motion of the running horse is irreversible, requiring the movement of its legs to align with the
 127 running direction. The method generates a natural motion of a running horse, while satisfying the
 128 boundary condition of the end frame. Similarly, the other irreversible motions are generated with
 129 realistic dynamics, such as air bubbles rising from a scuba diver. Based on this observation, we
 130 propose a novel autoregressive approach for bounded video generation, which aligns with the video
 131 model’s forward-generation bias. More experimental details are provided in Appendix.

132 3.2 Main method

133 3.2.1 Context-aware bidirectional autoregressive denoising

134 We introduce context-aware denoising method,
 135 inspired by Stein Variational Gradient De-
 136 scent (SVGD) [12, 15]. Specifically, SVGD
 137 provides the gradient for particle x to approximate
 138 target distribution p as follows:

$$\Delta x = \mathbf{E}_{x' \sim q(x')} [k(x, x') \nabla_{x'} \log p(x') + \nabla_{x'} k(x, x')] \quad (1)$$

139 For known distribution q , and positive definite ker-
 140 nel k . The SVGD provides a direction toward high-
 141 density region using the other particles x' , preventing
 142 collapse by pushing each other with the second term.

143 We suggest context-aware gradient, inspired by
 144 SVGD. For the video generation, closely located frames should exchange the score update more than
 145 the far one. Accordingly, we set q as the distribution of preceding frames in the same diffusion time
 146 step. Moreover, we exclude the second term, as the video model already prevents the collapse. For
 147 the DDIM where $z_t = \sqrt{\alpha_t} \hat{z} + \sqrt{1 - \alpha_t} \epsilon$, we present the gradient for forward direction, $\Delta z_{\mathcal{X}}$, in
 148 clean manifold as follows:

$$\Delta z_{\mathcal{X}}(i) := \sum_{j < i} g(i, j) \Delta \hat{z}_j \quad (2)$$

149 where i and j are frame indices, g is monotonic decreasing function for the frame distance, and $\Delta \hat{z}_j$
 150 is the predicted update of preceding frames z_j in clean manifold. The gradient for reverse direction
 151 $\Delta z_{\mathcal{Y}}$ is defined in similar way. For implementation, we update the gradients by moving average
 152 that satisfies g , as shown in Fig. 5. Thereby, $\Delta \hat{z}$ captures contextual information for each time step.
 153 Additionally, we apply DDS[25] to the frame for input context, to satisfy the boundary condition.

154 Then, we set time schedule to generate frames in both directions in autoregressive manner. As
 155 illustrated in Fig. 5, we add more noise in the direction of the generation, which is inspired by
 156 previous method[11, 18]. Specifically, the model ϕ denoises the sequence $\{z_f\}_{f=1}^F$, where each
 157 frame z_f has different diffusion time $\tau(f)$ as follows:

$$\tau(f) = \max\{f + (T - l_{CTX}), T\} \quad (3)$$

$$z_{f, \tau-1} = \phi(\{z_{f, \tau}\}_{f=1}^F, \{\tau(f)\}_{f=1}^F) \quad (4)$$

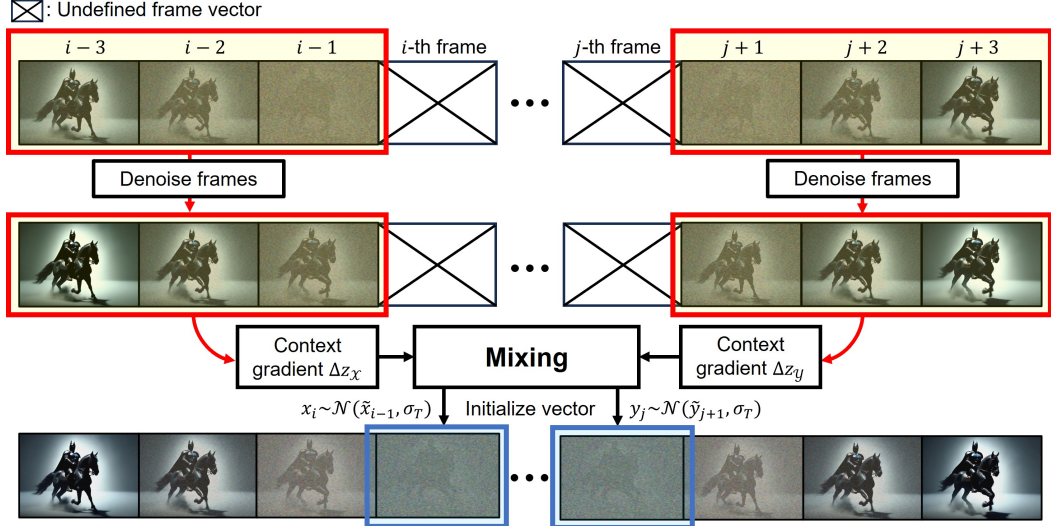


Figure 6: Overall diagram of proposed context-aware bidirectional generation. We extract the context gradient $\Delta z_{\mathcal{X}}, \Delta z_{\mathcal{Y}}$ from each sequence, and utilize them to generate the new frames.

158 where f is frame index, F is input frame length of model, l_{CTX} is the length of input context, and
 159 T is maximum number of time. Here, we denote a set of indices for each sequence as \mathcal{X} and \mathcal{Y} ,
 160 respectively. \mathcal{X} and \mathcal{Y} are updated for each denoising step by removing the index of fully denoised
 161 frame and adding the index of new frame. If there are no new frames to add, we apply lookahead
 162 denoising[11]. We provide details for the denoising process in the Appendix.

163 **3.2.2 Reducing context gap for coherent video**

164 In the proposed bidirectional generation method, main challenge becomes to address context gap
 165 between the forward and reversed frames. Specifically, as each direction retains its own frame context,
 166 discrete transition emerges in the middle when the two sequences are combined to generate bounded
 167 video. Hence, the interdependency between the two directions should be considered to generate
 168 coherent video. Accordingly, we propose a method for a smooth transition between the two sequences.
 169 Specifically, we propose the method for frame initialization, and the context gradient to guide frames
 170 to consider the context in global perspective. For clarity, in this section, we denote the diffusion
 171 vector z as x for forward direction, and y for the backward direction. First, we design the mixing
 172 ratio $R(i, j)$ which determines the ratio of information exchange between the two sequences in global
 173 view. Similarly, we define the frame kernel $k(i, j)$ to consider local context. Then, we initialize x_i
 174 using the predicted of frames in set \mathcal{X}, \mathcal{Y} , as follows:

$$\tilde{x}_{i-1} = (1 - r) \sum_{m \in \mathcal{X}} k(i, m) \hat{x}_m + r \sum_{n \in \mathcal{Y}} k(i, n) \hat{y}_n \quad (5)$$

$$x_i \sim \mathcal{N}(\tilde{x}_{i-1}, \sigma_T) \quad (6)$$

175 for maximum noise level σ_T , mixing ratio $r = R(i, j)$ and frame kernel k . Likewise, \hat{y}_j is sampled in
 176 similar way. It is simple, but effective, as the interpolation in the noisy manifold results the semantic
 177 interpolation in clean manifold[8, 16, 19]. Next, we suggest a context gradient which provides a
 178 guidance considering the global context. Following the linearity of equation (2), we obtain the context
 179 gradient as:

$$\Delta \tilde{x}_i = (1 - r) \Delta z_{\mathcal{X}} + r \Delta z_{\mathcal{Y}} \quad (7)$$

$$\Delta \tilde{y}_j = (1 - r) \Delta z_{\mathcal{Y}} + r \Delta z_{\mathcal{X}} \quad (8)$$

180 which provides guidance to each frame during diffusion process. To clarify our method, we present
 181 pseudo code in Algorithm 1.

Algorithm 1 Autoregressive generation for bounded video

Input: Forward set \mathcal{X} , reverse set \mathcal{Y} , frame latents $\{z_f\}_{f=0}^L$
Output: Denoised latents $\{z_f\}_{f=1}^{L-1}$, updated \mathcal{X}, \mathcal{Y}
// Bounded diagonal denoising //
1: Get time steps $\{\tau_f\}_{f=0}^L$
2: For $i \in \mathcal{X}$, predict $\{\hat{z}_i\} = \phi(\{z_i\}, \{\tau(i)\})$ using $\Delta\tilde{z}_i$
3: For $j \in \mathcal{Y}$, predict $\{\hat{z}_j\} = \phi(\{z_j\}, \{\tau(j)\})$ using $\Delta\tilde{z}_j$
4: Update $\tau(f)$
// Initialization of next frames i', j' //
5: Get $c_{\mathcal{X}} = \sum_{m \in \mathcal{X}} k(i', m) \hat{z}_m$, $c_{\mathcal{Y}} = \sum_{n \in \mathcal{Y}} k(j', n) \hat{z}_n$ and $r = R(i', j')$
6: $\tilde{z}_{i'-1} = (1 - r) c_{\mathcal{X}} + r c_{\mathcal{Y}}$
7: $\tilde{z}_{j'+1} = (1 - r) c_{\mathcal{Y}} + r c_{\mathcal{X}}$
8: Sample $z_{i'} \sim \mathcal{N}(\tilde{z}_{i'-1}, \sigma_T)$ and $z_{j'} \sim \mathcal{N}(\tilde{z}_{j'+1}, \sigma_T)$
9: Update gradients $\Delta z_{\mathcal{X}}, \Delta z_{\mathcal{Y}}$ by moving average
10: Add new indices: $\mathcal{X}.\text{add}(i')$, $\mathcal{Y}.\text{add}(j')$
11: **if** $\min \tau(f) = 0$ **then**
12: Output frames: z_0, z_L
13: Delete indices: $\mathcal{X}.\text{remove}(0), \mathcal{Y}.\text{remove}(L)$

182 **4 Experimental Results**183 **4.1 Implementation Details**

184 Our method requires an initial set of frames for input context, as we progressively generates video
185 frames. In our experiment, we generate a short video, and use it as an initial context. Our code is
186 based on the official implementation of FIFO². We compare our method with previous training-free
187 methods. First, we compare our method with FIFO[11], a state-of-art autoregressive method. Then,
188 we select TRF[5] and ViBiDSampler[25] which are recent methods for bounded video generation.
189 Specifically, we adjust the input frame length for TRF and ViBiDSampler, as the methods generates
190 whole frames at once, which are not the autoregressive manner. For the experiment of the bounded
191 video generation, we conducted experiments for two tasks, where the first task is generation of
192 looped video by identical bound, and the second task is the generation of smooth video by the two
193 bounds[5]. We randomly create 200 prompts by GPT-4[1] for each task. We utilized the publicly
194 release videocrafter2 [3] model for the experiments. The experiments are conducted by H100 GPUs.
195 For the comparison, we evaluate the videos in three aspects, temporal consistency, visual quality and
196 boundary satisfaction. We selected Temporal Flickering, Background Consistency in VBench [9] to
197 evaluate temporal smoothness, and FVD[20] and FID[7] to compare perceptual quality of frames.
198 For boundary satisfaction, we calculate mean absolute error (MAE) of frames in pixel space. More
199 details can be found in the Appendix.

200 **4.2 Bounded video generation**

201 We present the result of bounded video generation in Fig. 7, which demonstrates the superiority of our
202 method compared to the previous methods. First, for the experiment on identical bound, our method
203 successfully generates the looping video with high visual quality, while satisfying the input bounds.
204 Specifically, our method generates the detailed and realistic motion, such as splashing water and
205 natural movement of heron flapping the wings. In case of FIFO[11], the method results open-ended
206 video, which fails to satisfy the bound. In contrast, TRF[5] generates bounded videos following
207 the input bound. However, the output shows blurry texture and motion. Specifically, the texture of
208 splashing water and the motion of the wings become overly smooth. ViBiDSampler[25] outputs
209 finer details than TRF, but still blurry compared to our method. Here, the degradation in visual
210 quality arises from a mismatch of input sequence length used for training and inference, also shown
211 in previous work[17]. In contrast, our approach maintains the consistent length by autoregressive
212 approach, effectively avoiding the degradation.

²https://github.com/jjihwan/FIFO-Diffusion_public

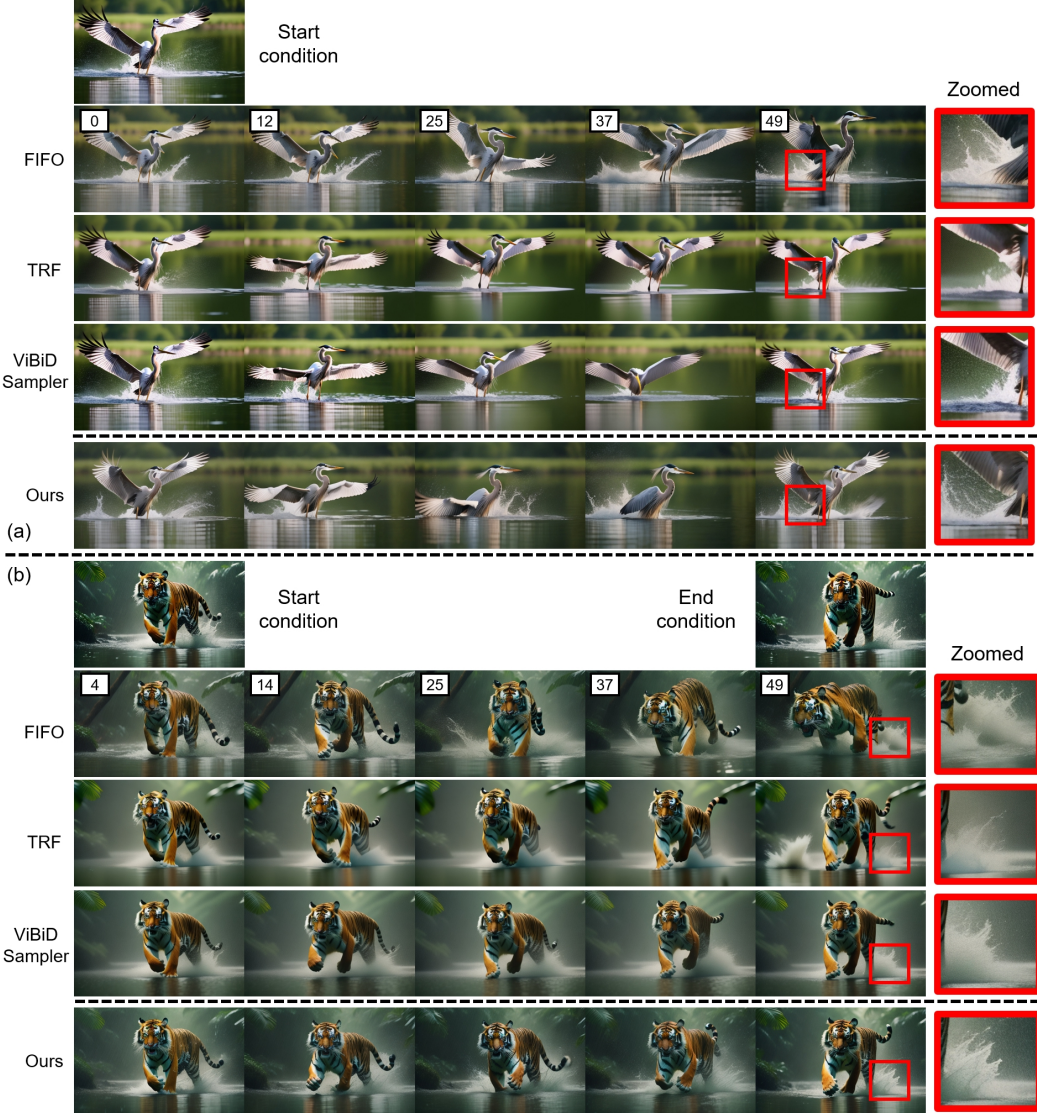


Figure 7: Main result of bounded video generation. (a) Looped video generation by identical bound. (b) Bounded video generation conditioned on two bounds, distinct start and end frames.

Table 1: Quantitative comparison for bounded video generation. Our method successfully generate bounded video with enhanced visual quality.

	Temporal Consistency		Visual quality		Boundary satisfaction		
	Temporal Flickering \uparrow	Background Consistency \uparrow	$FVD_{16} \downarrow$	$FID \downarrow$	MAE(Loop)	MAE(Start)	MAE(End)
TRF	0.957	0.966	591.44	52.75	0.066	0.137	0.122
ViBiD	0.952	0.967	429.28	35.59	0.074	0.139	0.114
FIFO	0.934	0.961	386.72	30.28	0.202	0.152	0.235
Ours	0.957	0.969	393.76	31.61	0.076	0.097	0.101

213 Second, for the experiment for two bounds, our method also outperforms the other method in terms
214 both of visual quality and boundary satisfaction. Our method shows detailed texture for both object
215 and background, specifically the texture of leaves in jungle and the splashing water. Moreover, our
216 method successfully generate frames in between two bounds with enhanced temporal consistency. On
217 the contrary, FIFO fails to satisfy the ending bound, as it generates frames autoregressively without
218 any constraints. In case of TRF, the result satisfies the bounds, maintaining the temporal coherent

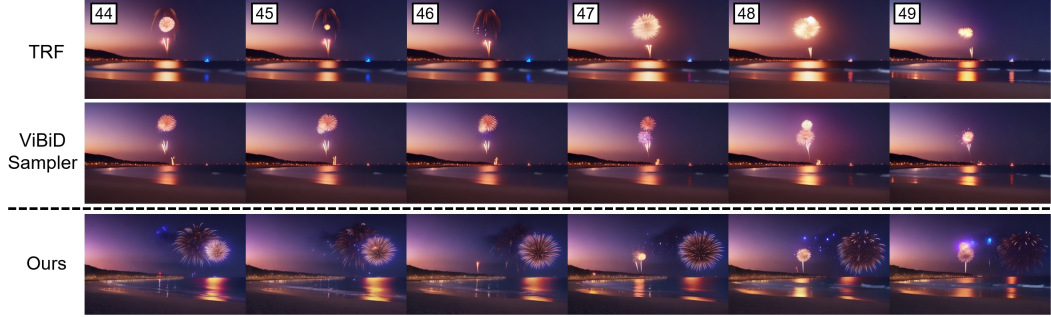


Figure 8: Comparison of irreversible motions in single bounded video with 50 frames. Numbers in the images indicate frame index. We present a typical irreversible motion, movement firework flares.



Figure 9: Ablation study for video length. We observe the deviation of context according to the length of video.

219 between the frames. However, the frames demonstrate low visual quality with smoothed texture,
 220 which is coherent result for looped video generation. Moreover, the method fails to generate the
 221 realistic motion of tiger. Likewise, ViBiDSampler results frames with better visual quality and motion
 222 than TRF, but worse than the proposed method. Both previous methods suffers from degraded visual
 223 quality due to the difference in input sequence length between training and inference. In contrast,
 224 the proposed autoregressive approach avoids the degradation by allowing the consistent input length.
 225 Overall, the results in both experiments demonstrates the superiority of our method.

226 Further, we provide quantitative comparison in Table 1. Compared to FIFO, our method outputs
 227 enhanced temporal consistency by considering the frame context. Moreover, boundary conditions are
 228 satisfied in our method, which is not in FIFO. Compared to TRF and ViBiDSampler, our method
 229 outputs better visual quality and boundary satisfaction.

230 4.3 Discussion

231 4.3.1 Irreversible motion

232 Our method leverages the video model’s bias when generating the reversed frames, whereas the
 233 previous methods are counter to the bias by flipping the frame. To support the claim, we present
 234 empirical evidence in Fig. 8. Specifically, we compare the frames near the end of video with
 235 irreversible motion, the flares in firework. Our method successfully generates the natural fading of
 236 firework flares. Whereas, TRF and ViBiDSampler output unnatural shrinkage of the flares, which are
 237 reversed dynamics. The results demonstrate the superiority of the proposed approach in generating
 238 realistic motions compared to the previous approach.

239 4.3.2 Video length

240 Our method generates frames in an autoregressive manner, enabling the generation of bounded videos
 241 of arbitrary length. However, as the video length increases, the generated frames gradually deviate
 242 from initial boundary frames. Accordingly, we further explore the deviation of context as the length
 243 of video increases. As shown in Fig. 9, we conduct the ablation study on video lengths for looped
 244 video generation. In the case of a short video with 20 frames, the generated frames maintain the
 245 initial context of input image, preserving the background and overall scene. However, for a longer
 246 video with 100 frames, a gradual shift in context is observed. Specifically, as the frames progress, the
 247 dancing couple dominates the scene where the stage gradually changes with the emerge of focused

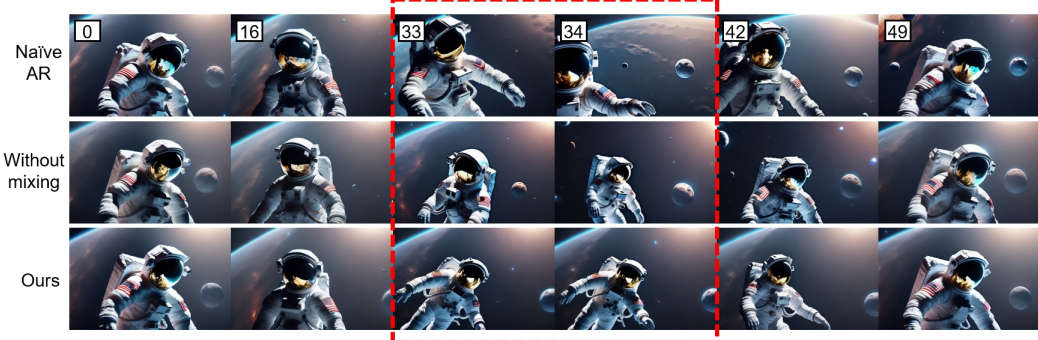


Figure 10: Output frames to explore context gap. Abrupt change between intermediate frames is observed in the middle of video caused by the context gap. Red rectangle highlights the discontinuity.

248 lighting. Despite the deviation, the frames gradually reconstructs the original scene in the end. The
 249 results demonstrate that generation of long video accompanies the contextual shifts by the weakened
 250 long-range dependency. Additionally, it is notable that our method successfully generates a coherent
 251 bounded video even in the presence of the deviation.

252 4.3.3 Context gap

253 To evaluate the effectiveness of the proposed
 254 method, we conduct an ablation study exploring the
 255 context gap in the output video with single bound.
 256 We compare our method with two variants, one with-
 257 out consideration of global context ('Without mix-
 258 ing') and another using a naive combination of diffu-
 259 sion time schedules for forward and backward gen-
 260 eration ('Naive AR'). Compared to Naive AR, the
 261 consideration of context improves temporal con-
 262 sistency in both directions, as shown in Fig. 10. How-
 263 ever, a discontinuity emerges in the middle, where
 264 the transition occurs between the sequences. This
 265 is caused by the context gap of the two directions,
 266 leading to abrupt changes in motion and background.
 267 In contrast, our method successfully resolves the dis-
 268 continuity, showing the consistent video frames.

269 For the quantitative comparison, we measure mean absolute error (MAE) between intermediate
 270 frames. As shown in Fig. 11, three videos shows similar trends of MAE in gray region, as they follow
 271 the given bound. However, each method shows distinct tendency after the bound. Considering the
 272 context enhances the temporal consistency, lowering the MAE. However, a large peak emerges in
 273 the middle, which indicates the context gap between the two directions. When the mixing is applied,
 274 the peak is removed, which indicates a smooth transition. The results demonstrate that our method
 275 successfully outputs coherent bounded video, effectively mitigating the context gap.

276 5 Conclusion

277 We proposed a novel bidirectional autoregressive approach for bounded video generation. First, we
 278 suggest context-aware autoregressive denoising which generates frames in both forward and reversed
 279 directions, effectively leveraging the video model's forward generation bias. Moreover, we introduce
 280 the context gradient to capture the contextual information of frames. Then, we propose a novel
 281 method, to reduce the context gap between the two directions. Our method is capable of generating
 282 bounded videos of arbitrary length while satisfying the boundary conditions. Experimental results
 283 verify the outperformance of our method compared to the related methods. Moreover, we present
 284 inherent limitation of previous approach by comparing the results for irreversible motion. We further
 285 conduct the ablation studies to validate the effectiveness of each component in our method.

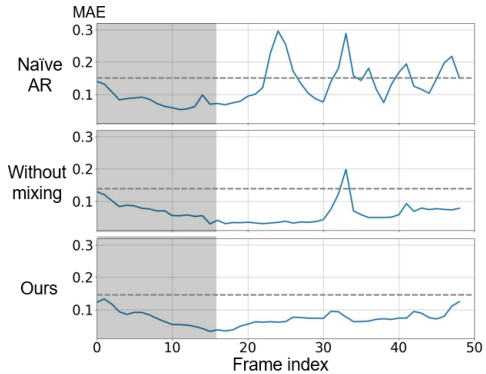


Figure 11: MAE between frames. Gray region indicates the input bound frames.

286 **References**

287 [1] Josh Achiam, Steven Adler, Sandhini Agarwal, Lama Ahmad, Ilge Akkaya, Florencia Leoni Aleman,
288 Diogo Almeida, Janko Altenschmidt, Sam Altman, Shyamal Anadkat, et al. Gpt-4 technical report. *arXiv*
289 *preprint arXiv:2303.08774*, 2023.

290 [2] Andreas Blattmann, Tim Dockhorn, Sumith Kulal, Daniel Mendelevitch, Maciej Kilian, Dominik Lorenz,
291 Yam Levi, Zion English, Vikram Voleti, Adam Letts, et al. Stable video diffusion: Scaling latent video
292 diffusion models to large datasets. *arXiv preprint arXiv:2311.15127*, 2023.

293 [3] Haoxin Chen, Yong Zhang, Xiaodong Cun, Menghan Xia, Xintao Wang, Chao Weng, and Ying Shan.
294 Videocrafter2: Overcoming data limitations for high-quality video diffusion models. In *Proceedings of the*
295 *IEEE/CVF Conference on Computer Vision and Pattern Recognition*, pages 7310–7320, 2024.

296 [4] Hyungjin Chung, Suhyeon Lee, and Jong Chul Ye. Decomposed diffusion sampler for accelerating
297 large-scale inverse problems. In *The Twelfth International Conference on Learning Representations*, 2024.

298 [5] Haiwen Feng, Zheng Ding, Zhihao Xia, Simon Niklaus, Victoria Abrevaya, Michael J Black, and Xuaner
299 Zhang. Explorative inbetweening of time and space. In *European Conference on Computer Vision*, pages
300 378–395. Springer, 2024.

301 [6] Yoav HaCohen, Nisan Chiprut, Benny Brazowski, Daniel Shalem, Dudu Moshe, Eitan Richardson, Eran
302 Levin, Guy Shiran, Nir Zabari, Ori Gordon, et al. Ltx-video: Realtime video latent diffusion. *arXiv*
303 *preprint arXiv:2501.00103*, 2024.

304 [7] Martin Heusel, Hubert Ramsauer, Thomas Unterthiner, Bernhard Nessler, and Sepp Hochreiter. Gans
305 trained by a two time-scale update rule converge to a local nash equilibrium. *Advances in neural information*
306 *processing systems*, 30, 2017.

307 [8] Jonathan Ho, Ajay Jain, and Pieter Abbeel. Denoising diffusion probabilistic models. *Advances in neural*
308 *information processing systems*, 33:6840–6851, 2020.

309 [9] Ziqi Huang, Yinan He, Jiashuo Yu, Fan Zhang, Chenyang Si, Yuming Jiang, Yuanhan Zhang, Tianxing Wu,
310 Qingyang Jin, Nattapol Chanpaisit, et al. Vbench: Comprehensive benchmark suite for video generative
311 models. In *Proceedings of the IEEE/CVF Conference on Computer Vision and Pattern Recognition*, pages
312 21807–21818, 2024.

313 [10] Yang Jin, Zhicheng Sun, Ningyuan Li, Kun Xu, Hao Jiang, Nan Zhuang, Quzhe Huang, Yang Song,
314 Yadong Mu, and Zhouchen Lin. Pyramidal flow matching for efficient video generative modeling. *arXiv*
315 *preprint arXiv:2410.05954*, 2024.

316 [11] Jihwan Kim, Junoh Kang, Jinyoung Choi, and Bohyung Han. Fifo-diffusion: Generating infinite videos
317 from text without training. *Advances in Neural Information Processing Systems*, 37:89834–89868, 2025.

318 [12] Subin Kim, Kyungmin Lee, June Suk Choi, Jongheon Jeong, Kihyuk Sohn, and Jinwoo Shin. Collaborative
319 score distillation for consistent visual editing. In *Thirty-seventh Conference on Neural Information*
320 *Processing Systems*, 2023.

321 [13] Weijie Kong, Qi Tian, Zijian Zhang, Rox Min, Zuozhuo Dai, Jin Zhou, Jiangfeng Xiong, Xin Li, Bo Wu,
322 Jianwei Zhang, et al. Hunyuandvideo: A systematic framework for large video generative models. *arXiv*
323 *preprint arXiv:2412.03603*, 2024.

324 [14] Bin Lin, Yunyang Ge, Xinhua Cheng, Zongjian Li, Bin Zhu, Shaodong Wang, Xianyi He, Yang Ye,
325 Shenghai Yuan, Liuhan Chen, et al. Open-sora plan: Open-source large video generation model. *arXiv*
326 *preprint arXiv:2412.00131*, 2024.

327 [15] Qiang Liu and Dilin Wang. Stein variational gradient descent: A general purpose bayesian inference
328 algorithm. *Advances in neural information processing systems*, 29, 2016.

329 [16] Chenlin Meng, Yutong He, Yang Song, Jiaming Song, Jiajun Wu, Jun-Yan Zhu, and Stefano Ermon. Sdedit:
330 Guided image synthesis and editing with stochastic differential equations. *arXiv preprint arXiv:2108.01073*,
331 2021.

332 [17] Haonan Qiu, Menghan Xia, Yong Zhang, Yingqing He, Xintao Wang, Ying Shan, and Ziwei Liu. Freenoise:
333 Tuning-free longer video diffusion via noise rescheduling. *arXiv preprint arXiv:2310.15169*, 2023.

334 [18] David Ruhe, Jonathan Heek, Tim Salimans, and Emiel Hoogeboom. Rolling diffusion models. In
335 *Proceedings of the 41st International Conference on Machine Learning*, pages 42818–42835. PMLR,
336 2024.

337 [19] Jiaming Song, Chenlin Meng, and Stefano Ermon. Denoising diffusion implicit models. *arXiv preprint arXiv:2010.02502*, 2020.

338 [20] Thomas Unterthiner, Sjoerd Van Steenkiste, Karol Kurach, Raphael Marinier, Marcin Michalski, and Sylvain Gelly. Towards accurate generative models of video: A new metric & challenges. *arXiv preprint arXiv:1812.01717*, 2018.

342 [21] Vikram Voleti, Alexia Jolicoeur-Martineau, and Chris Pal. Mcvd-masked conditional video diffusion for prediction, generation, and interpolation. *Advances in neural information processing systems*, 35: 23371–23385, 2022.

345 [22] Fu-Yun Wang, Wenshuo Chen, Guanglu Song, Han-Jia Ye, Yu Liu, and Hongsheng Li. Gen-l-video: Multi-text to long video generation via temporal co-denoising. *arXiv preprint arXiv:2305.18264*, 2023.

347 [23] Xiaojuan Wang, Boyang Zhou, Brian Curless, Ira Kemelmacher-Shlizerman, Aleksander Holynski, and Steve Seitz. Generative inbetweening: Adapting image-to-video models for keyframe interpolation. In *The Thirteenth International Conference on Learning Representations*, 2025.

350 [24] Jinbo Xing, Menghan Xia, Yong Zhang, Haoxin Chen, Wangbo Yu, Hanyuan Liu, Gongye Liu, Xintao Wang, Ying Shan, and Tien-Tsin Wong. Dynamicrafter: Animating open-domain images with video diffusion priors. In *European Conference on Computer Vision*, pages 399–417. Springer, 2024.

353 [25] Serin Yang, Taesung Kwon, and Jong Chul Ye. Vibidsampler: Enhancing video interpolation using bidirectional diffusion sampler. *arXiv preprint arXiv:2410.05651*, 2024.

355 [26] Shengming Yin, Chenfei Wu, Huan Yang, Jianfeng Wang, Xiaodong Wang, Minheng Ni, Zhengyuan Yang, Linjie Li, Shuguang Liu, Fan Yang, et al. Nuwa-xl: Diffusion over diffusion for extremely long video generation. *arXiv preprint arXiv:2303.12346*, 2023.

358 **A Additional results**

359 We provide additional results for both identical bound and dynamic bound in Fig. 12 and Fig. 13. Our
360 method successfully generates the bounded video with high quality while satisfying the boundary
361 condition.

362 **B Experimental settings**

363 **B.1 Key observation**

364 We present autoregressive reversed frame generation as key observation in the main paper. The
365 implementation of the experiment is based on the publicly released code of FIFO³, which generates
366 open-ended video in forward direction by autoregressive manner. Accordingly, the hyperparameters
367 are identical to the baseline. For the experiment to generate the reverse direction, we reversed two
368 key components in FIFO[11], the time schedule and a direction of lookahead denoising. We utilized
369 publicly released video model, videocrafter2[3]. The experiments are conducted by H100 GPUs.
370 The text conditions for the Figure 4 in main paper are "A dark knight riding horse in glass land" and
371 "scubar diver exploring the shipwreck underwater", which are selected to visualize the successful
372 generation of irreversible motions in reversed direction.

373 **B.2 Proposed method**

374 We follow the experimental setting of TRF[5] which suggests three categories for bounded video
375 generation task. Specifically, for single bound task, we generate a video conditioned on a text
376 prompt and set as the bound. For two bound task, following 'Dynamic Bound' in TRF, we sample
377 frames from the generated video with moving object. For the prompts in Fig. 7 in main paper, we
378 used "Cinematic photo of a heron taking off in slow motion from still water" for single bound, and
379 "Cinematic photo of a tiger charging through dense jungle in a monsoon, leaves and water flying with
380 each step" for two bounds.

381 **Hyperparameters**

382 Our implementation is based on implementation of FIFO. Hence, we share the hyperparameters and
383 settings with the baseline. DDIM[19] schedule with 64 inference steps is utilized. The length of
384 videos is 50 frames, unless specified. We defined the frame kernel $k(i, j)$ and mixing ratio $R(i, j)$ as
385 gaussian kernel. Specifically, each function is defined as follows:

$$k(i, j) = c_k \exp\{-(i - j)^2 / \gamma_k\} \quad (9)$$

$$R(i, j) = \lambda_R c_R \exp\{-(i - j)^2 / L\gamma_R\} \quad (10)$$

386 where $\gamma_k, \gamma_R, \lambda_R$ are the hyperparameter, L is the total length of video sequence. c_k and c_R are
387 the normalizing constant. In our method, each parameters are set as $\gamma_k = 16, \gamma_R = 4, \lambda_R = 0.5$.
388 Specifically, $k(i, j)$ has a length of 16 and is normalized so that the sum of each element becomes
389 one. The weight to update Δz by moving average is set as 0.6 for single bound, and 0.8 for two
390 bounds.

391 **Evaluation metric**

392 We evaluate videos in three different perspective, which are temporal consistency, visual quality
393 of frames and satisfaction of the given boundary. To evaluate the temporal consistency, we utilize
394 the temporal flickering and background consistency suggested in VBench[9], which calculate the
395 difference between frames in mean absolute error(MAE) using pixel values and CLIP features,
396 respectively. Specifically, in both metrics, higher value indicates more smoothness in video, where
397 the maximum value is 1.

398 To evaluate the visual quality, we present FVD_{16} [17, 20] and FID[7]. Specifically, following the
399 previous work[17], we compare the output with input context of 16 frames, sampling the 16 frames
400 in the generated video. For FID, we calculate the metric between the input bound frames and the
401 output frames. We calculate the metric using 400 generated videos, where the prompts are randomly
402 generated by GPT-4[1].

³https://github.com/jjihwan/FIFO-Diffusion_public



Figure 12: Additional result for looped video with identical bound. The selected frame indices are {0, 12, 25, 37, 49}

403 To evaluate the boundary satisfaction, we simply calculated the MAE difference of frames in pixel
 404 space. Specifically, for the looped video with single bound, we calculate the MAE between the first
 405 frame and the last frame. In case of bounded video with two different bounds, we calculate the MAE
 406 for the start condition, as the difference between the last context frame and the first generated frame.
 407 For instance, the last context frame is 16 and the other one is 17, for the input context length of 16 in
 408 the generated video. Then, we obtain the MAE for end condition, as the difference between the last
 409 frame of generated video and the first frame of the end context. The values are normalized with the
 410 maximum pixel value, 255. Lower value indicates better boundary satisfaction.

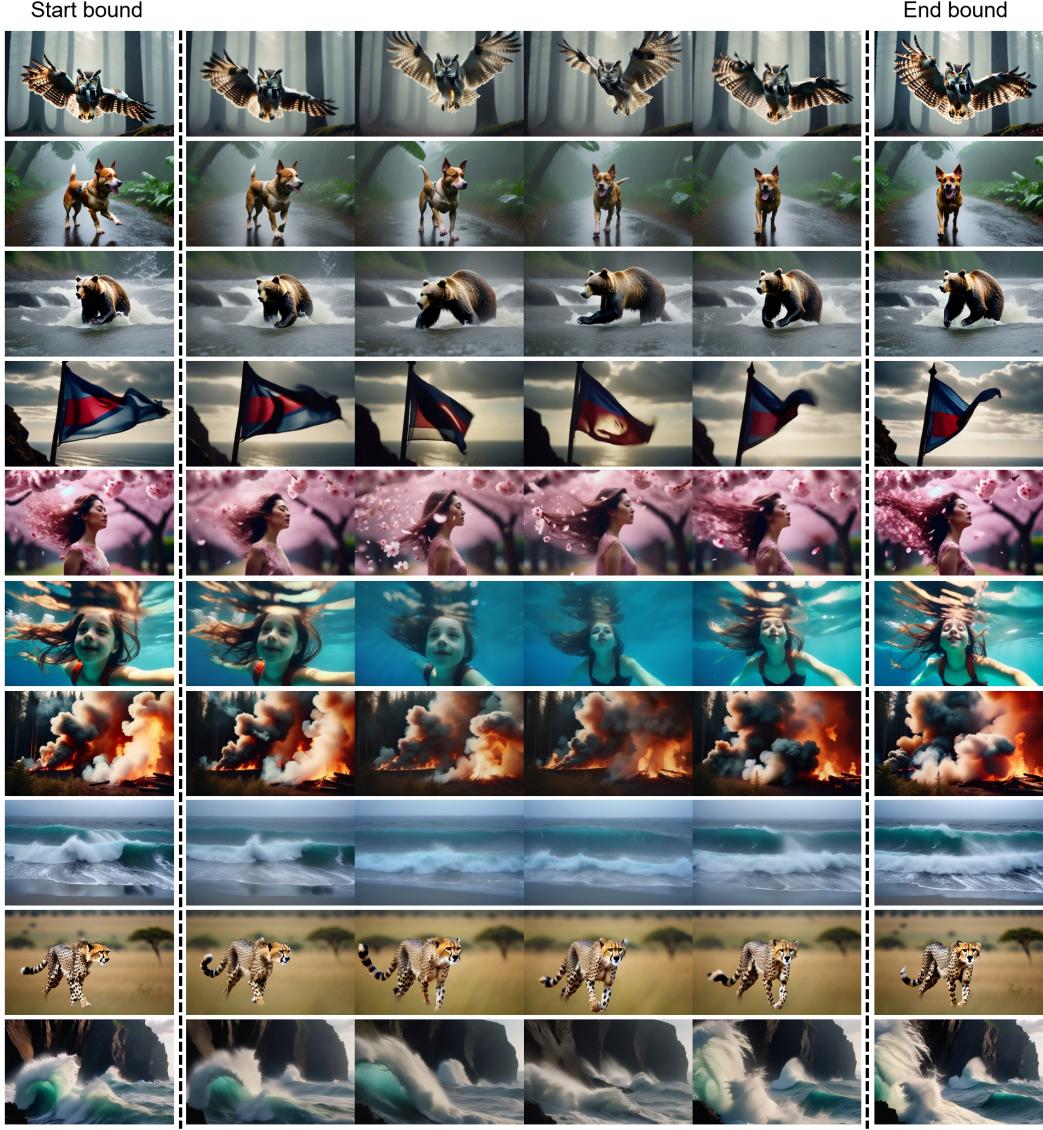


Figure 13: Additional result for looped video with dynamic bound. The selected frame indices are $\{4, 19, 34, 49\}$

411 **C Denoising process**

412 **C.1 Inference stages**

413 Our method has three different phases for video generation, since the sequence length gradually
 414 shortens as generated frames are removed from both sides. We provide a detailed explanation of each
 415 phase.

416 **Phase 1: No overlaps between \mathcal{X} and \mathcal{Y}**

417 In this phase, we consistently add new frames to each set, \mathcal{X} and \mathcal{Y} . The new frames are initialized
 418 by the mixing of frame predictions, as described in the main paper. If the size of \mathcal{X} and \mathcal{Y} exceed the
 419 model’s input frame length, lookahead denoising is applied independently to each side. We do not
 420 alternate the direction of lookahead denoising in this phase.

421

422 **Phase 2: No more new frames**

423 In this phase, there is no more new frame to initialize. Now, we apply alternating lookahead



Figure 14: Lookahead denoising in both forward and reverse direction for bounded video generation. In our method, we apply the lookahead denoising only once for each denoising step, alternating the direction for each diffusion step.

424 denoising suggested in Section D, to denoise the sequence while considering the generation bias for
 425 both directions.

426

427 **Phase 3: Sequence shorter than model input size**

428 In this phase, lookahead denoising is no longer applied, as the sequence can be denoised without the
 429 latent partitioning. Generated frames are not removed from the sequence. Instead, they are input to
 430 the model along with the remaining noisy frames, to provide the model an additional information.
 431 The generated frames are not updated, as they already completed the diffusion generation process.

432 **D Lookahead denoising**

433 We utilized lookahead denoising along with the latent partitioning to make noise prediction be more
 434 accurate, as suggested in the previous method, FIFO. Specifically, as shown forward partitions in
 435 Fig. 14, the sequence is separated by several partitions to reduce the noise level difference between
 436 the intermediate frames. Moreover, lookahead denoising is utilized to further improve the accuracy of
 437 noise prediction, as the model predicts the noise, considering the cleaner frames.

438 For bounded video generation in our work, we utilize lookahead denoising in both the forward and
 439 reverse directions. Specifically, as illustrated in Fig. 14, we alternate the direction of lookahead
 440 denoising at each step of the diffusion process. Lookahead denoising impose the generation bias to
 441 align frames with the respect of direction of denoising. By leveraging both directions, our method
 442 improves the temporal consistency of the generated bounded video.

443 **E Limitations and Potential negative impact**

444 Our method preserves the context to generate coherent bounded video by the mixing strategy.
 445 Therefore, if there is big content difference between the bounds, the output video may presents
 446 degraded transition between the two sequences. For the social impact, as most of generative methods
 447 share, the video generation by the proposed work may induce a social disinformation by creating
 448 realistic fake videos. Moreover, there is risk of generating videos with harmful contents.

449 **NeurIPS Paper Checklist**

450 **1. Claims**

451 Question: Do the main claims made in the abstract and introduction accurately reflect the
452 paper's contributions and scope?

453 Answer: **[Yes]**

454 Justification: The paper clarifies the contribution of our research in the abstract and the
455 introduction.

456 Guidelines:

- 457 • The answer NA means that the abstract and introduction do not include the claims
458 made in the paper.
- 459 • The abstract and/or introduction should clearly state the claims made, including the
460 contributions made in the paper and important assumptions and limitations. A No or
461 NA answer to this question will not be perceived well by the reviewers.
- 462 • The claims made should match theoretical and experimental results, and reflect how
463 much the results can be expected to generalize to other settings.
- 464 • It is fine to include aspirational goals as motivation as long as it is clear that these goals
465 are not attained by the paper.

466 **2. Limitations**

467 Question: Does the paper discuss the limitations of the work performed by the authors?

468 Answer: **[Yes]**

469 Justification: We present the discussion on the limitation in Section E.

470 Guidelines:

- 471 • The answer NA means that the paper has no limitation while the answer No means that
472 the paper has limitations, but those are not discussed in the paper.
- 473 • The authors are encouraged to create a separate "Limitations" section in their paper.
- 474 • The paper should point out any strong assumptions and how robust the results are to
475 violations of these assumptions (e.g., independence assumptions, noiseless settings,
476 model well-specification, asymptotic approximations only holding locally). The authors
477 should reflect on how these assumptions might be violated in practice and what the
478 implications would be.
- 479 • The authors should reflect on the scope of the claims made, e.g., if the approach was
480 only tested on a few datasets or with a few runs. In general, empirical results often
481 depend on implicit assumptions, which should be articulated.
- 482 • The authors should reflect on the factors that influence the performance of the approach.
483 For example, a facial recognition algorithm may perform poorly when image resolution
484 is low or images are taken in low lighting. Or a speech-to-text system might not be
485 used reliably to provide closed captions for online lectures because it fails to handle
486 technical jargon.
- 487 • The authors should discuss the computational efficiency of the proposed algorithms
488 and how they scale with dataset size.
- 489 • If applicable, the authors should discuss possible limitations of their approach to
490 address problems of privacy and fairness.
- 491 • While the authors might fear that complete honesty about limitations might be used by
492 reviewers as grounds for rejection, a worse outcome might be that reviewers discover
493 limitations that aren't acknowledged in the paper. The authors should use their best
494 judgment and recognize that individual actions in favor of transparency play an impor-
495 tant role in developing norms that preserve the integrity of the community. Reviewers
496 will be specifically instructed to not penalize honesty concerning limitations.

497 **3. Theory assumptions and proofs**

498 Question: For each theoretical result, does the paper provide the full set of assumptions and
499 a complete (and correct) proof?

500 Answer: **[NA]**

501 Justification: The paper does not include any theoretical results.

502 Guidelines:

- 503 • The answer NA means that the paper does not include theoretical results.
- 504 • All the theorems, formulas, and proofs in the paper should be numbered and cross-
505 referenced.
- 506 • All assumptions should be clearly stated or referenced in the statement of any theorems.
- 507 • The proofs can either appear in the main paper or the supplemental material, but if
508 they appear in the supplemental material, the authors are encouraged to provide a short
509 proof sketch to provide intuition.
- 510 • Inversely, any informal proof provided in the core of the paper should be complemented
511 by formal proofs provided in appendix or supplemental material.
- 512 • Theorems and Lemmas that the proof relies upon should be properly referenced.

513 4. Experimental result reproducibility

514 Question: Does the paper fully disclose all the information needed to reproduce the main ex-
515 perimental results of the paper to the extent that it affects the main claims and/or conclusions
516 of the paper (regardless of whether the code and data are provided or not)?

517 Answer: [Yes]

518 Justification: We present detailed experimental settings in Section 4.1 and Section B.

519 Guidelines:

- 520 • The answer NA means that the paper does not include experiments.
- 521 • If the paper includes experiments, a No answer to this question will not be perceived
522 well by the reviewers: Making the paper reproducible is important, regardless of
523 whether the code and data are provided or not.
- 524 • If the contribution is a dataset and/or model, the authors should describe the steps taken
525 to make their results reproducible or verifiable.
- 526 • Depending on the contribution, reproducibility can be accomplished in various ways.
527 For example, if the contribution is a novel architecture, describing the architecture fully
528 might suffice, or if the contribution is a specific model and empirical evaluation, it may
529 be necessary to either make it possible for others to replicate the model with the same
530 dataset, or provide access to the model. In general, releasing code and data is often
531 one good way to accomplish this, but reproducibility can also be provided via detailed
532 instructions for how to replicate the results, access to a hosted model (e.g., in the case
533 of a large language model), releasing of a model checkpoint, or other means that are
534 appropriate to the research performed.
- 535 • While NeurIPS does not require releasing code, the conference does require all submis-
536 sions to provide some reasonable avenue for reproducibility, which may depend on the
537 nature of the contribution. For example
 - 538 (a) If the contribution is primarily a new algorithm, the paper should make it clear how
539 to reproduce that algorithm.
 - 540 (b) If the contribution is primarily a new model architecture, the paper should describe
541 the architecture clearly and fully.
 - 542 (c) If the contribution is a new model (e.g., a large language model), then there should
543 either be a way to access this model for reproducing the results or a way to reproduce
544 the model (e.g., with an open-source dataset or instructions for how to construct
545 the dataset).
 - 546 (d) We recognize that reproducibility may be tricky in some cases, in which case
547 authors are welcome to describe the particular way they provide for reproducibility.
548 In the case of closed-source models, it may be that access to the model is limited in
549 some way (e.g., to registered users), but it should be possible for other researchers
550 to have some path to reproducing or verifying the results.

551 5. Open access to data and code

552 Question: Does the paper provide open access to the data and code, with sufficient instruc-
553 tions to faithfully reproduce the main experimental results, as described in supplemental
554 material?

Answer: [No]

Justification: We provide pseudo code in Section 3.2 and detailed settings in Section B, to support the reproducibility of our method. In case of code, we will release it publicly after the acceptance, due to the internal rules regarding on intellectual property of our institution.

Guidelines:

- The answer NA means that paper does not include experiments requiring code.
- Please see the NeurIPS code and data submission guidelines (<https://nips.cc/public/guides/CodeSubmissionPolicy>) for more details.
- While we encourage the release of code and data, we understand that this might not be possible, so “No” is an acceptable answer. Papers cannot be rejected simply for not including code, unless this is central to the contribution (e.g., for a new open-source benchmark).
- The instructions should contain the exact command and environment needed to run to reproduce the results. See the NeurIPS code and data submission guidelines (<https://nips.cc/public/guides/CodeSubmissionPolicy>) for more details.
- The authors should provide instructions on data access and preparation, including how to access the raw data, preprocessed data, intermediate data, and generated data, etc.
- The authors should provide scripts to reproduce all experimental results for the new proposed method and baselines. If only a subset of experiments are reproducible, they should state which ones are omitted from the script and why.
- At submission time, to preserve anonymity, the authors should release anonymized versions (if applicable).
- Providing as much information as possible in supplemental material (appended to the paper) is recommended, but including URLs to data and code is permitted.

6. Experimental setting/details

Question: Does the paper specify all the training and test details (e.g., data splits, hyper-parameters, how they were chosen, type of optimizer, etc.) necessary to understand the results?

Answer: [Yes]

Justification: We provide details in experimental settings in Section 4.1 and Section B.

Guidelines:

- The answer NA means that the paper does not include experiments.
- The experimental setting should be presented in the core of the paper to a level of detail that is necessary to appreciate the results and make sense of them.
- The full details can be provided either with the code, in appendix, or as supplemental material.

7. Experiment statistical significance

Question: Does the paper report error bars suitably and correctly defined or other appropriate information about the statistical significance of the experiments?

Answer: [No]

Justification: Error bars are not presented, as it requires large computational resources.

Guidelines:

- The answer NA means that the paper does not include experiments.
- The authors should answer "Yes" if the results are accompanied by error bars, confidence intervals, or statistical significance tests, at least for the experiments that support the main claims of the paper.
- The factors of variability that the error bars are capturing should be clearly stated (for example, train/test split, initialization, random drawing of some parameter, or overall run with given experimental conditions).
- The method for calculating the error bars should be explained (closed form formula, call to a library function, bootstrap, etc.)
- The assumptions made should be given (e.g., Normally distributed errors).

607 • It should be clear whether the error bar is the standard deviation or the standard error
 608 of the mean.
 609 • It is OK to report 1-sigma error bars, but one should state it. The authors should
 610 preferably report a 2-sigma error bar than state that they have a 96% CI, if the hypothesis
 611 of Normality of errors is not verified.
 612 • For asymmetric distributions, the authors should be careful not to show in tables or
 613 figures symmetric error bars that would yield results that are out of range (e.g. negative
 614 error rates).
 615 • If error bars are reported in tables or plots, The authors should explain in the text how
 616 they were calculated and reference the corresponding figures or tables in the text.

617 **8. Experiments compute resources**

618 Question: For each experiment, does the paper provide sufficient information on the com-
 619 puter resources (type of compute workers, memory, time of execution) needed to reproduce
 620 the experiments?

621 Answer: [\[Yes\]](#)

622 Justification: We clarify the type of GPUs for the experiment in Section 4.1.

623 Guidelines:

624 • The answer NA means that the paper does not include experiments.
 625 • The paper should indicate the type of compute workers CPU or GPU, internal cluster,
 626 or cloud provider, including relevant memory and storage.
 627 • The paper should provide the amount of compute required for each of the individual
 628 experimental runs as well as estimate the total compute.
 629 • The paper should disclose whether the full research project required more compute
 630 than the experiments reported in the paper (e.g., preliminary or failed experiments that
 631 didn't make it into the paper).

632 **9. Code of ethics**

633 Question: Does the research conducted in the paper conform, in every respect, with the
 634 NeurIPS Code of Ethics <https://neurips.cc/public/EthicsGuidelines>?

635 Answer: [\[Yes\]](#)

636 Justification: Our work follows the NeurIPS Code of Ethics.

637 Guidelines:

638 • The answer NA means that the authors have not reviewed the NeurIPS Code of Ethics.
 639 • If the authors answer No, they should explain the special circumstances that require a
 640 deviation from the Code of Ethics.
 641 • The authors should make sure to preserve anonymity (e.g., if there is a special consid-
 642 eration due to laws or regulations in their jurisdiction).

643 **10. Broader impacts**

644 Question: Does the paper discuss both potential positive societal impacts and negative
 645 societal impacts of the work performed?

646 Answer: [\[Yes\]](#)

647 Justification: We provide the discussion on the societal impacts in Section E

648 Guidelines:

649 • The answer NA means that there is no societal impact of the work performed.
 650 • If the authors answer NA or No, they should explain why their work has no societal
 651 impact or why the paper does not address societal impact.
 652 • Examples of negative societal impacts include potential malicious or unintended uses
 653 (e.g., disinformation, generating fake profiles, surveillance), fairness considerations
 654 (e.g., deployment of technologies that could make decisions that unfairly impact specific
 655 groups), privacy considerations, and security considerations.

656 • The conference expects that many papers will be foundational research and not tied
 657 to particular applications, let alone deployments. However, if there is a direct path to
 658 any negative applications, the authors should point it out. For example, it is legitimate
 659 to point out that an improvement in the quality of generative models could be used to
 660 generate deepfakes for disinformation. On the other hand, it is not needed to point out
 661 that a generic algorithm for optimizing neural networks could enable people to train
 662 models that generate Deepfakes faster.
 663 • The authors should consider possible harms that could arise when the technology is
 664 being used as intended and functioning correctly, harms that could arise when the
 665 technology is being used as intended but gives incorrect results, and harms following
 666 from (intentional or unintentional) misuse of the technology.
 667 • If there are negative societal impacts, the authors could also discuss possible mitigation
 668 strategies (e.g., gated release of models, providing defenses in addition to attacks,
 669 mechanisms for monitoring misuse, mechanisms to monitor how a system learns from
 670 feedback over time, improving the efficiency and accessibility of ML).

671 **11. Safeguards**

672 Question: Does the paper describe safeguards that have been put in place for responsible
 673 release of data or models that have a high risk for misuse (e.g., pretrained language models,
 674 image generators, or scraped datasets)?

675 Answer: **[No]**

676 Justification: Our work do not release any data or models.

677 Guidelines:

- 678 • The answer NA means that the paper poses no such risks.
- 679 • Released models that have a high risk for misuse or dual-use should be released with
 680 necessary safeguards to allow for controlled use of the model, for example by requiring
 681 that users adhere to usage guidelines or restrictions to access the model or implementing
 682 safety filters.
- 683 • Datasets that have been scraped from the Internet could pose safety risks. The authors
 684 should describe how they avoided releasing unsafe images.
- 685 • We recognize that providing effective safeguards is challenging, and many papers do
 686 not require this, but we encourage authors to take this into account and make a best
 687 faith effort.

688 **12. Licenses for existing assets**

689 Question: Are the creators or original owners of assets (e.g., code, data, models), used in
 690 the paper, properly credited and are the license and terms of use explicitly mentioned and
 691 properly respected?

692 Answer: **[Yes]**

693 Justification: We properly credited and clarified the licenses of the models in section 4.1.

694 Guidelines:

- 695 • The answer NA means that the paper does not use existing assets.
- 696 • The authors should cite the original paper that produced the code package or dataset.
- 697 • The authors should state which version of the asset is used and, if possible, include a
 698 URL.
- 699 • The name of the license (e.g., CC-BY 4.0) should be included for each asset.
- 700 • For scraped data from a particular source (e.g., website), the copyright and terms of
 701 service of that source should be provided.
- 702 • If assets are released, the license, copyright information, and terms of use in the
 703 package should be provided. For popular datasets, paperswithcode.com/datasets
 704 has curated licenses for some datasets. Their licensing guide can help determine the
 705 license of a dataset.
- 706 • For existing datasets that are re-packaged, both the original license and the license of
 707 the derived asset (if it has changed) should be provided.

708 • If this information is not available online, the authors are encouraged to reach out to
709 the asset's creators.

710 **13. New assets**

711 Question: Are new assets introduced in the paper well documented and is the documentation
712 provided alongside the assets?

713 Answer: **[No]**

714 Justification: After acceptance, we will provide the documented details when we release the
715 code.

716 Guidelines:

717 • The answer NA means that the paper does not release new assets.

718 • Researchers should communicate the details of the dataset/code/model as part of their
719 submissions via structured templates. This includes details about training, license,
720 limitations, etc.

721 • The paper should discuss whether and how consent was obtained from people whose
722 asset is used.

723 • At submission time, remember to anonymize your assets (if applicable). You can either
724 create an anonymized URL or include an anonymized zip file.

725 **14. Crowdsourcing and research with human subjects**

726 Question: For crowdsourcing experiments and research with human subjects, does the paper
727 include the full text of instructions given to participants and screenshots, if applicable, as
728 well as details about compensation (if any)?

729 Answer: **[NA]**

730 Justification: Our experiments are not related to human subject.

731 Guidelines:

732 • The answer NA means that the paper does not involve crowdsourcing nor research with
733 human subjects.

734 • Including this information in the supplemental material is fine, but if the main contribu-
735 tion of the paper involves human subjects, then as much detail as possible should be
736 included in the main paper.

737 • According to the NeurIPS Code of Ethics, workers involved in data collection, curation,
738 or other labor should be paid at least the minimum wage in the country of the data
739 collector.

740 **15. Institutional review board (IRB) approvals or equivalent for research with human
741 subjects**

742 Question: Does the paper describe potential risks incurred by study participants, whether
743 such risks were disclosed to the subjects, and whether Institutional Review Board (IRB)
744 approvals (or an equivalent approval/review based on the requirements of your country or
745 institution) were obtained?

746 Answer: **[NA]**

747 Justification: Our experiments are not related to human subject.

748 Guidelines:

749 • The answer NA means that the paper does not involve crowdsourcing nor research with
750 human subjects.

751 • Depending on the country in which research is conducted, IRB approval (or equivalent)
752 may be required for any human subjects research. If you obtained IRB approval, you
753 should clearly state this in the paper.

754 • We recognize that the procedures for this may vary significantly between institutions
755 and locations, and we expect authors to adhere to the NeurIPS Code of Ethics and the
756 guidelines for their institution.

757 • For initial submissions, do not include any information that would break anonymity (if
758 applicable), such as the institution conducting the review.

759 **16. Declaration of LLM usage**

760 Question: Does the paper describe the usage of LLMs if it is an important, original, or
761 non-standard component of the core methods in this research? Note that if the LLM is used
762 only for writing, editing, or formatting purposes and does not impact the core methodology,
763 scientific rigorousness, or originality of the research, declaration is not required.

764 Answer: [Yes]

765 Justification: As our method is targeting for text-conditioned video generation, we employ
766 LLM to randomly generate the motion instructions, as clarified in section 4.1.

767 Guidelines:

768 • The answer NA means that the core method development in this research does not
769 involve LLMs as any important, original, or non-standard components.
770 • Please refer to our LLM policy (<https://neurips.cc/Conferences/2025/LLM>)
771 for what should or should not be described.